JACS
JOURNAL OF THE AMERICAN CHEMICAL SOCIETY
pubs.acs.org/JACS
Communication

Atomic-Scale Structure of Chemically Distinct Surface Oxygens in Redox Reactions

Anusheela Das, Haesun Park, Yanna Chen, Devika Choudhury, Tien-Lin Lee, Jeffrey W. Elam, Peter Zapol, and Michael J. Bedzyk*

Cite This: J. Am. Chem. Soc. 2021, 143, 17937−17941
Read Online
ACCESS | Metrics & More | Article Recommendations | Supporting Information

ABSTRACT: During redox reactions, oxide-supported catalytic systems undergo structural and chemical changes. Improving subsequent catalytic properties requires an understanding of the atomic-scale structure with chemical state specificity under reaction conditions. For the case of 1/2 monolayer vanadia on α-TiO_2(110), we use X-ray standing wave (XSW) excited X-ray photoelectron spectroscopy to follow the redox induced atomic positional and chemical state changes of this interface. While the resulting XSW 3D composite atomic maps include the Ti and O substrate atoms and V surface atoms, our focus in this report is on the previously unseen surface oxygen species with comparison to density functional theory predictions.

Oxide-supported catalysts are very commonly used in the chemical industry and in pollution abatement. Several reactions such as hydrogenation, transesterification, and dehydrogenation have increased efficiency with supported metal-oxide catalysts compared to using bulk catalysts. The use of a supported catalyst reduces the amount needed and increases the active surface area, thus decreasing cost and enhancing chemical activity of the catalyst. In this work we study one such system, TiO_2 supported vanadium oxide, which is widely used for selective catalytic reduction of NOx and catalytic oxidation of organic compounds.[1−4]

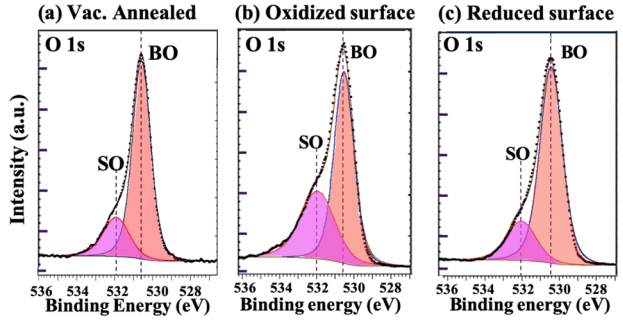

Figure 1. O 1s XP spectra at 1.9 keV incident energy for the (a) vacuum annealed surface, (b) oxidized surface, and (c) reduced surface.

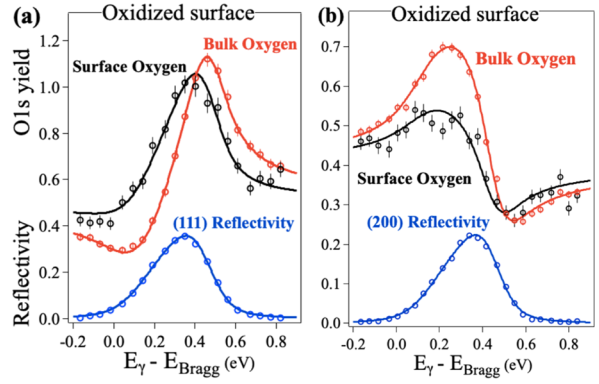

Figure 2. Modulations in BO and SO XPS yields for the oxidized surface from the energy scans through the (a) (111) and (b) (200) reflections.

We discuss a novel model-independent 3D atomic mapping technique, which follows the change in surface site locations of chemically distinct surface atoms during a redox reaction. This method, XSW excited XPS,[5−7] is uniquely suited for locating surface oxygen atoms, which are distinguished from oxygens in the supporting oxide substrate, by a chemical shift to their binding energy. This is an extension to earlier studies which used XSW excited X-ray fluorescence (XRF) measurements to create element specific atomic maps.[8,9] For the presented case of 1/2 monolayer (ML) vanadium on α-TiO_2(110), the interface between the support and the catalyst plays a major role in controlling the structure and in turn the activity of the catalyst. The surface oxygen atoms take part in the catalytic reaction, and hence their positions are modified during the process. Herein, we use the XSW-XPS method to directly observe in situ reversible structural and chemical state modifications of the VOx/α-TiO_2(110) interface. This is combined with density functional theory (DFT) calculations[10−12] to further improve and extend our understanding of this complex catalytic system.

Received: July 29, 2021
Published: October 21, 2021

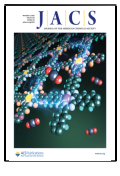

https://doi.org/10.1021/jacs.1c07926
J. Am. Chem. Soc. 2021, 143, 17937−17941

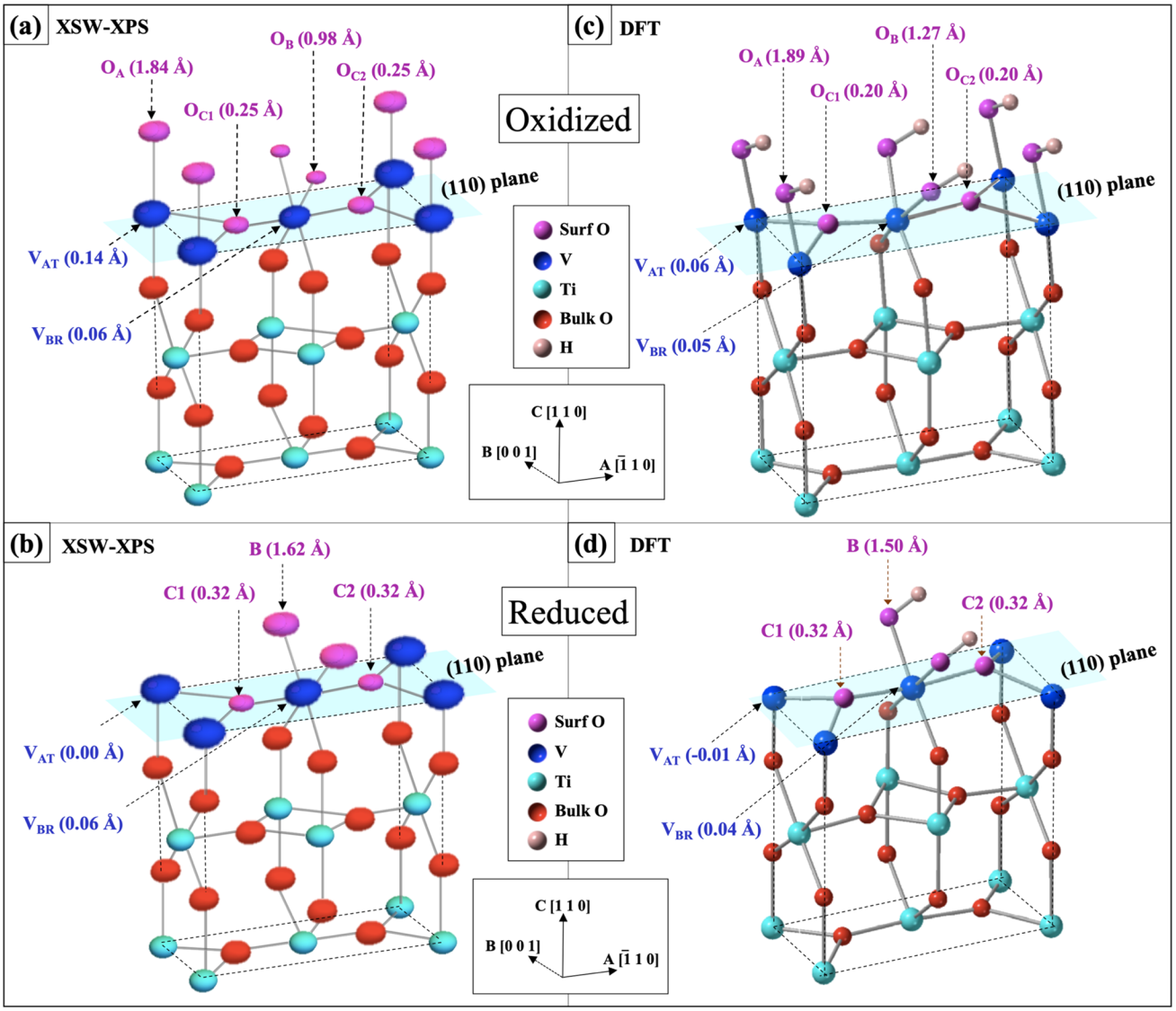

Figure 3. (a, b) XSW-XPS determined model-independent composite atomic maps of SO, BO, V, and bulk Ti for (a) oxidized and (b) reduced surface. The size of each V and SO oval is proportional to its fractional occupancy. (c, d) DFT calculated model for (c) oxidized and (d) reduced surface.

Atomic layer deposition (ALD) was used to grow 1/2 ML of VO_x on a rutile α-TiO_2 (110) surface (1 ML = 10.4 atoms/nm^2). After transport to the ultrahigh vacuum (UHV) chamber at the I09 Diamond Light Source X-ray station, the sample was annealed at 350 °C to clean and reduce the surface. This was followed by dosing the surface with atomic O and then H from a thermal gas cracker cell to create the oxidized or reduced surfaces, respectively, for in situ redox studies (see the Supporting Information for details). Ex situ atomic force microscopy before and after film growth and after the reactions showed atomically flat terraces separated by atomic steps (Figure S3). Low-energy electron diffraction of the rutile TiO_2 (110) surface before and after the growth of submonolayer vanadia and after the reactions showed (1 × 1) patterns (Figure S3). Back-reflection XSW-XPS[3,13] was used at I09 to measure the distributions of interfacial atoms relative to the substrate TiO_2 lattice with both subangstrom spatial resolution and chemical state specificity. The XSW, which is generated by dynamical Bragg diffraction from the substrate crystal, extends above and below the surface and has a period equal to the *d*-spacing of the **H** = *hkl* diffraction planes. Analysis of the XSW induced modulation to a photoemission signal determines the amplitude (f_H) and phase (P_H) of the *H*th Fourier component of the spatial distribution for that emitter (see the Supporting Information for details). One specular (110) and three off-specular (101, 111, 200) XSW data sets were collected to triangulate the atomic positions in 3D. Each set of *hkl* measurements were repeated after each redox treatment to study the dynamic changes in the surface structure under in situ reaction conditions.

In agreement with previous results for similar surfaces,[4,8,10,14] the XP spectra in Figure 1 show that the O 1s photoelectrons experience roughly 1.5 eV higher binding energy when emitted from surface oxygens (SO) than from bulk oxygens (BO).[15,16] Grazing emission XPS measurements compared to nongrazing emission, shown in Figure S4, confirms that these SO atoms are at the surface. Density functional theory (DFT) calculations indicate that these SO atoms are partially hydroxylated. Based on the integrated peak areas estimated from Figure 1, the vacuum annealed surface

https://doi.org/10.1021/jacs.1c07926
J. Am. Chem. Soc. 2021, 143, 17937−17941

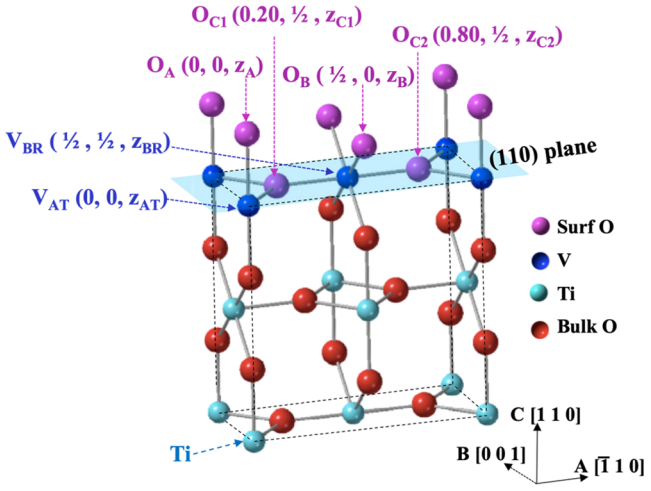

Figure 4. Depiction of the (110) termination of a rutile α-TiO_2 crystal showing three symmetry inequivalent surface oxygens (A, B, C). Also shown are the surface Ti atop (AT) and bridging (BR) sites, which are partially occupied by V atoms. The dotted lines outline a conveniently chosen nonprimitive tetragonal unit cell with its *C*-axis perpendicular to the TiO_2 (110) surface. See Figure S9 for more details.

Table 1. Oxidized Surface: XSW Determined Best Fit Vertical Heights of Surface Oxygens (SO) above the Bulk TiO (110) Plane and Heights Obtained from DFT; Also Listed Is the Fraction of SO at Each Site (42% of the SO Atoms Are Uncorrelated)

site	exptl *Z* (Å)	DFT *Z* (Å)	α
A	1.84 (3)	1.89	0.23
B	0.98 (3)	1.27	0.03
C1	0.25 (3)	0.20	0.16
C2	0.25 (3)	0.20	0.16

Table 2. Reduced Surface: XSW Determined Best Fit Vertical Heights of SO and Heights Obtained from DFT; Also Listed Is the Fraction of SO at Each Site (50% of the SO Atoms Are Uncorrelated)

site	exptl *Z* (Å)	DFT *Z* (Å)	α
A			0.00
B	1.62 (3)	1.50	0.32
C1	0.32 (3)	0.32	0.09
C2	0.32 (3)	0.32	0.09

had 0.50 ML, oxidized surface 0.88 ML, and reduced surface 0.44 ML of SO atoms. While DFT calculations were primarily used to optimize structures, the DFT calculations are also in general agreement with the XP spectra, predicting a chemical shift of 1.3 eV for hydroxylated SO on V and 1.0 eV on Ti as shown in Figures S17 and S19 (see the Supporting Information for details).

The in situ XSW measurements induced distinctive modulations for these two O 1s XPS peaks from scans across four reflections. The XSW data and analysis are shown in Figures 2a,b and Figures S12–S15 with the resulting four sets of f_H and P_H measured values for each chemical state of oxygen listed in Tables S4–S6. A Fourier summation of these four sets of Fourier components and their symmetry equivalents is then used to generate model-independent 3D atomic density $\rho(\mathbf{r})$ maps.[17−22]

$$\rho(\boldsymbol{r}) = 1 + 2 \sum_{\substack{H \neq -H \\ H \neq 0}} f_H \cos[2\pi(P_H - \mathbf{H}\cdot\mathbf{r})] \quad (1)$$

Because there is a signal from each type of atom at this interface, we combine these maps into a 3D composite atomic map. Using the Ti 2p, V 2p, bulk O 1s, and surface O 1s XSW-XPS results, we show such composite maps for the oxidized and reduced surfaces in Figures 3a and 3b, respectively. The initial vacuum annealed surface, discussed in the Supporting Information, has a 3D map (Figure S16) similar to that of the reduced surface. For all three surfaces, the bulk Ti and O show up in their expected positions in the composite maps and show no redox induced changes.

For the oxidized surface, the V cations, which are 64% V^{5+} and 36% V^{4+}, laterally occupy 32% of the atop (AT) sites and 24% of the bridging (BR) sites with heights above the TiO (110) bulk-like plane listed in Figure 3a. The chemically shifted surface oxygens show up at the A, B, and C sites with heights as indicated in Figure 3a. The oxidized surface DFT model (Figure 3c) shows good agreement with these experimentally determined V and SO heights.

For the reduced surface, chemically shifted surface oxygens are detected at the B and C sites, but not at the A site (Figure 3b). The DFT (Figure 3d) is in good agreement showing no A-site oxygen and closely agreeing with the XSW experimental heights for B and C sites. V ions are 78% V^{4+} and 22% V^{5+} for the reduced surface and occupy 44% of the AT and 42% of the BR. Because the initial vacuum annealed surface had a similar composite 3D map as the reduced surface, we would conclude that the redox process was reversible for this surface.

To improve our understanding of this complex system, we created a three-site model illustrated in Figure 4 to quantitatively analyze the experimental data. The model, which is based on the model-independent 3D atomic maps, partitions the surface O to laterally sit at A, B, and C sites or to be uncorrelated to the substrate lattice. (There are two symmetry equivalent C-sites, C1 and C2.) To quantify the structural parameters associated with these three adsorption sites, we performed a least-squares global fit of this model to the experimentally measured f_H and P_H values for each redox condition. Here, the *H*th Fourier component for the SO atomic distribution is defined as

$$F_H = f_H e^{i2\pi P_H} = \alpha_A e^{i2\pi \mathbf{H}\cdot\mathbf{r}_A} + \alpha_B e^{i2\pi \mathbf{H}\cdot\mathbf{r}_B} + \alpha_{C1} e^{i2\pi \mathbf{H}\cdot\mathbf{r}_{C1}} + \alpha_{C2} e^{i2\pi \mathbf{H}\cdot\mathbf{r}_{C2}} \quad (2)$$

where α_X denotes the fraction of surface O occupying site X = *A*, *B*, *C*1, and *C*2 with positions $\mathbf{r}_A = (00z_A)$, $\mathbf{r}_B = (^1/_2 0 z_B)$, $\mathbf{r}_{C1} = (0.2^1/_2 z_{C1})$, and $\mathbf{r}_{C2} = (0.8^1/_2 z_{C2})$. z_x is the height of O above the TiO (110) bulk-like plane (Figure 4). The global fits of eq 2 to the sets of measured f_H and P_H values give α and z at each SO site. Table 1 for the Ox and Table 2 for the Re surface list the heights above the (110) plane of TiO_2 (in Å) by using $Z = zC$, where $C = 2d_{110} = 6.496$ Å. The tables also list the heights obtained from the DFT calculations for comparison. Also listed are the eq 2 determined values of α for SO. The Supporting Information shows various calculations to prove consistency between the model-independent, model-dependent, and DFT results. The XSW-XPS analysis of the V 2p for these same oxidized and reduced surfaces will be the focus of a subsequent paper.

https://doi.org/10.1021/jacs.1c07926
J. Am. Chem. Soc. 2021, 143, 17937−17941

We see from Tables 1 and 2 that SO atoms in B and C positions are shifted upward on the reduced surface compared to the oxidized one. Both experiment and DFT calculations show the same trend. This suggests that the reduced charge on V ions leads to weakening of ionic interactions between V and SO, resulting in elongation of V−O bonds. To gain further insights into the SO behavior, several different oxidized and reduced surface models were evaluated by using DFT calculations to optimize the structures. The best agreement with the SO vertical positions for the reduced surface is obtained for the model structure shown in Figure 3d, where the V ions are in isomorphic positions with the rutile substrate and surface oxygens in the VO layer are partially hydrogenated. The presence of H atoms determines the vertical height of V at the BR site where the V atom shifts upward from the bulk-like Ti position; however, the absence of such a terminal O atom at A site keeps the vertical position of AT-site V unchanged as seen from both XSW measurements and DFT calculations. Based on these results, a possible interpretation of the reduced surface structure is the formation of 2D islands of hydrogenated VO_2 coherent with TiO_2.

Upon oxidation, surface oxygens show up at all four possible sites in the surface periodic cell as seen in Figures 3a and 3c. Comparing experiment and DFT results, we see similar shifts in the heights at each site. The presence of H at both A and B sites results in V at both AT and BR sites to be shifted upward. Also, as seen from DFT, the amount of chemically shifted oxygens on the oxidized surface is twice that on the reduced surface, which agrees with the coverage calculated from experiment shown in Figure 1. Thus, the XSW experiment and DFT calculations agree for the various chemically distinct surface oxygen atoms and V atoms in both reduced and oxidized surfaces. It is very interesting to observe that both DFT and XSW show that reduction removes only the A-site oxygen. This can be interpreted as the A-site being the catalytically active site.

In conclusion, we studied a supported vanadium oxide, demonstrating chemical-state-specific atomic-scale analysis for the redox-driven cation dynamics, under reversible oxidation and reduction processes. XSW-XPS analysis allowed us to generate 3D composite atomic density maps that show surface O atoms distinct from the bulk oxygens along with surface V and bulk Ti atoms. These observations are in good agreement with the DFT calculations. Such an approach can be applied to a broad range of reactions on functionalized crystalline surfaces.

■ ASSOCIATED CONTENT

Supporting Information

The Supporting Information is available free of charge at https://pubs.acs.org/doi/10.1021/jacs.1c07926.

Description of experimental setups and procedures, results, calculation parameters, DFT calculations, schematics, supplementary tables and figures (PDF)

■ AUTHOR INFORMATION

Corresponding Author

Michael J. Bedzyk − *Department of Materials Science and Engineering, Northwestern University, Evanston, Illinois 60208, United States; Department of Physics and Astronomy, Northwestern University, Evanston, Illinois 60208, United States;* orcid.org/0000-0002-1026-4558; Email: bedzyk@northwestern.edu

Authors

Anusheela Das − *Department of Materials Science and Engineering, Northwestern University, Evanston, Illinois 60208, United States*

Haesun Park − *Materials Science Division, Argonne National Laboratory, Lemont, Illinois 60439, United States; School of Integrative Engineering, Chung-Ang University, Seoul 06974, Republic of Korea*

Yanna Chen − *Department of Materials Science and Engineering, Northwestern University, Evanston, Illinois 60208, United States;* orcid.org/0000-0001-7937-4395

Devika Choudhury − *Applied Materials Division, Argonne National Laboratory, Lemont, Illinois 60439, United States*

Tien-Lin Lee − *Diamond Light Source, Harwell Science and Innovation Campus, Didcot OX11 0DE, United Kingdom*

Jeffrey W. Elam − *Applied Materials Division, Argonne National Laboratory, Lemont, Illinois 60439, United States;* orcid.org/0000-0002-5861-2996

Peter Zapol − *Materials Science Division, Argonne National Laboratory, Lemont, Illinois 60439, United States;* orcid.org/0000-0003-0570-9169

Complete contact information is available at: https://pubs.acs.org/10.1021/jacs.1c07926

Notes

The authors declare no competing financial interest.

■ ACKNOWLEDGMENTS

This research was supported by the U.S. Department of Energy, Office of Science, Office of Basic Energy Sciences, ICEP program, under Award DE-FG02-03ER15457. This work made use of the Keck-II facility and SPID facility of Northwestern University's NUANCE Center, which has received support from the SHyNE Resource (NSF ECCS-2025633), IIN, and Northwestern's MRSEC program (NSF DMR-1720139). This BRXSW-XPS work used Diamond Light Source (DLS) beamline I09 (DLS proposal number SI15748). The XRF V coverage measurement used DND-CAT at the Advanced Photon Source (APS). The ALD and use of the APS at Argonne National Lab are funded by DOE (DE-AC02-06CH11357). DFT work (H.P. and P.Z.) is supported by Laboratory Directed Research and Development (LDRD) funding from Argonne National Laboratory, provided by the Director, Office of Science, of the U.S. Department of Energy under Contract DE-AC02-06CH11357. We thank David McCue (DLS), Dr. Pardeep Thakur (DLS), and Dr. David Duncan (DLS) for assistance with our beamtime at DLS. We thank Dr. Anil Mane (ANL) for his help with ALD growth.

■ REFERENCES

(1) Wachs, I. E. Catalysis science of supported vanadium oxidecatalysts. *Dalton Trans* **2013**, *42*, 11762−11769.

(2) Kim, T.; Wachs, I. E. CH3OH oxidation over well-defined supported V2O5/Al2O3 catalysts: Influence of vanadium oxide loading and surface vanadium − oxygen functionalities. *J. Catal.* **2008**, *255*, 197−205.

(3) Kroger, E. A.; Allegretti, F.; Knight, M. J.; Polcik, M.; Sayago, D. I.; Woodruff, D. P.; Dhanak, V. R. Structural characterisation of ultra-thin VOx films on TiO_2(1 1 0). *Surf. Sci.* **2006**, *600*, 4813−4824.

(4) Kim, C.-Y.; Elam, J. W.; Stair, P. C.; Bedzyk, M. J. Redox Driven Crystalline Coherent-Incoherent Transformation for a 2 ML VOx

Film Grown on α-TiO_2(110). *J. Phys. Chem. C* **2010**, *114*, 19723−19726.
(5) Woodruff, D. P. Surface structure determination using x-ray standing waves: a simple view. *Rep. Prog. Phys.* **2005**, *68*, 743−798.
(6) Zegenhagen, J. Surface structure determination with X-ray standing waves. *Surf. Sci. Rep.* **1993**, *18*, 202−271.
(7) Solokha, V.; Garai, D.; Wilson, A.; Duncan, D. A.; Thakur, P. K.; Hingerl, K.; Zegenhagen, J. Water Splitting on Ti-Oxide-Terminated SrTiO3(001). *J. Phys. Chem. C* **2019**, *123* (28), 17232−17238.
(8) Feng, Z.; Cheng, L.; Kim, C.-Y.; Elam, J. W.; Zhang, Z.; Curtiss, L. A.; Zapol, P.; Bedzyk, M. J. Atomic-Scale Study of Ambient-Pressure Redox-Induced Changes for an Oxide-Supported Submonolayer Catalyst: VOx/α-TiO_2(110). *J. Phys. Chem. Lett.* **2012**, *3*, 2845−2850.
(9) Feng, Z.; Lu, J.; Feng, H.; Stair, P. C.; Elam, J. W.; Bedzyk, M. J. Catalysts Transform While Molecules React: An Atomic-Scale View. *J. Phys. Chem. Lett.* **2013**, *4*, 285−291.
(10) Benkoula, S.; Sublemontier, O.; Patanen, M.; Nicolas, C.; Sirotti, F.; Naitabdi, A.; Gaie-Levrel, F.; Antonsson, E.; Aureau, D.; Ouf, F.-X.; Wada, S.-I.; Etcheberry, A.; Ueda, K.; Miron, C. Water adsorption on TiO_2 surfaces probed by soft X-ray spectroscopies: bulk materials vs. isolated nanoparticles. *Sci. Rep.* **2015**, *5*, 15088.
(11) Köhler, L.; Kresse, G. Density functional study of CO on Rh(111). *Phys. Rev. B: Condens. Matter Mater. Phys.* **2004**, *70*, 165405.
(12) Kolczewski, C.; Hermann, K.; Guimond, S.; Kuhlenbeck, H.; Freund, H.-J. Identification of the vanadyl terminated V2O3(0 0 0 1) surface by NEXAFS spectroscopy: A combined theoretical and experimental study. *Surf. Sci.* **2007**, *601*, 5394−5402.
(13) Campbell, G. P.; Mannix, A. J.; Emery, J. D.; Lee, T.-L.; Guisinger, N. P.; Hersam, M. C.; Bedzyk, M. J. Resolving the Chemically Discrete Structure of Synthetic Borophene Polymorphs. *Nano Lett.* **2018**, *18*, 2816−2821.
(14) Hugenschmidt, M. B.; Gamble, L.; Campbell, C. T. The interaction of H_2O with a TiO_2(110) surface. *Surf. Sci.* **1994**, *302*, 329−340.
(15) Bagus, P. S.; Nelin, C. J.; Levchenko, S. V.; Zhao, X.; Davis, E. M.; Kuhlenbeck, H.; Freund, H.-J. Surface core level BE shifts for CaO(100): insights into physical origins. *Phys. Chem. Chem. Phys.* **2019**, *21*, 25431.
(16) Bagus, P. S.; Nelin, C. J.; Zhao, X.; Levchenko, S. V.; Davis, E.; Weng, X.; Späth, F.; Papp, C.; Kuhlenbeck, H.; Freund, H.-J. Revisiting surface core-level shifts for ionic compounds. *Phys. Rev. B: Condens. Matter Mater. Phys.* **2019**, *100*, 115419.
(17) Bedzyk, M. J.; Fenter, P. XSW Imaging. In *The X-Ray Standing Wave Technique: Principles and Applications*; Zegenhagen, J., Kazimirov, A., Eds.; World Scientific: Singapore, 2013; pp 289−302.
(18) Bedzyk, M. J.; Fenter, P.; Zhang, Z.; Cheng, L.; Okasinski, J. S.; Sturchio, N. C. Xray Standing Wave Imaging. *Synchrotron Radiation News* **2004**, *17*, 5−10.
(19) Cheng, L.; Fenter, P.; Bedzyk, M. J.; Sturchio, N. C. Fourier-expansion solution of atom distributions in a crystal using x-ray standing waves. *Phys. Rev. Lett.* **2003**, *90*, 255503.
(20) Kim, C. Y.; Elam, J. W.; Pellin, M. J.; Goswami, D. K.; Christensen, S. T.; Hersam, M. C.; Stair, P. C.; Bedzyk, M. J. Imaging of atomic layer deposited (ALD) tungsten monolayers on α-TiO_2(110) by X-ray standing wave Fourier inversion. *J. Phys. Chem. B* **2006**, *110*, 12616−12620.
(21) Lee, T.-L.; Bihler, C.; Schoch, W.; Limmer, W.; Daeubler, J.; Thieß, S.; Brandt, M. S.; Zegenhagen, J. Fourier transform imaging of impurities in the unit cells of crystals: Mn in GaAs. *Phys. Rev. B: Condens. Matter Mater. Phys.* **2010**, *81*, 235207.
(22) Meier, M.; Jakub, Z.; Balajka, J.; Hulva, J.; Bliem, R.; Thakur, P. K.; Lee, T.-L.; Franchini, C.; Schmid, M.; Diebold, U.; Allegretti, F.; Duncan, D. A.; Parkinson, G. S. Probing the geometry of copper and silver adatoms on magnetite: quantitative experiment versus theory. *Nanoscale* **2018**, *10*, 2226−2230.

https://doi.org/10.1021/jacs.1c07926
J. Am. Chem. Soc. 2021, 143, 17937−17941